Amplified-Spontaneous-Emission Spectrum of the Radiation Field in Surface-Emitting DFB Lasers

Ali M. Shams-Zadeh-Amiri, *Member, IEEE*, Wei Li, *Member, IEEE*, Hans Wenzel, and Xun Li, *Senior Member, IEEE*

***Abstract*—In this paper, the authors calculate the amplified-spontaneous-emission spectrum of the radiation field in surface-emitting distributed feedback (DFB) lasers. The response of the laser cavity to the Langevin noise source in the frequency domain is obtained using the newly developed Green's functions for the slowly varying amplitudes of the guided waves. The authors show that the power spectra from the surface and the edge are different, and this discrepancy is due to excitation of the radiation field by the interference between the counter-propagating waves inside the cavity. This feature can be properly exploited in the design of surface-emitting DFB lasers for optical communications.**

***Index Terms*—Amplified spontaneous emission (ASE), below-threshold spectrum, coupled-mode equations, DFB lasers, frequency-domain approach, grating-coupled surface-emitting lasers, Green's function, Langevin force, power spectrum, second-order gratings, spontaneous emission.**

I. Introduction

In SECOND-ORDER distributed feedback (DFB) lasers with index grating, radiation loss determines the mode selection, and the mode with less radiation loss is dominant [1], [2]. In these structures, the radiation field of the main mode is due to destructive interference between the counter-propagating waves forming that mode and has a concave near-field intensity pattern with a minimum at the center of the cavity [3]. Therefore, the radiation efficiency is reduced, and most of the radiated power is emitted from the regions close to the laser facets. Moreover, the corresponding far-field intensity pattern is double lobe. Up until now, different approaches have been proposed to modify the laser beam and overcome this inherent problem in second-order DFB lasers. These approaches are all based on tailoring the complex amplitudes of the guided waves inside the cavity [4]–[11].

Despite all efforts spent on the engineering of the laser beam in surface-emitting DFB lasers, to the best of our knowledge, the theoretical study of the surface-emitted power spectra has not yet been reported in the literature. In this paper, we address the below-threshold spectrum of the radiation power in surface-emitting DFB lasers with a second-order grating. We show that the relative intensities between the main mode and first side mode emitted from the surface and edge are different. This discrepancy is due to excitation of the radiation field by the interference between the guided waves inside the laser cavity. As will be shown later, if one compares the amplified-spontaneous-emission (ASE) spectra from the surface and the edge in a DFB laser with a second-order index grating, one may see that the relative intensity between the main mode and first side mode emitted from the surface is less than that from the edge. This issue is the result of destructive (constructive) interference between the guided waves forming the main mode (first side mode) and reduces the side-mode suppression ratio (SMSR) of the surface-emitted power compared to the SMSR of the power emitted from the edge. Therefore, this feature explains why conventional second-order DFB lasers with index grating may not be suitable for optical communications. We will also show that the opposite holds true, if the main mode is due to constructive interference between the guided waves.

We use the newly developed Green's functions for obtaining the response of the cavity to the Langevin noise source in the frequency domain [12]. Unlike the Green's function proposed by Henry [13], these new Green's functions relate the slowly varying amplitudes of the guided waves to the spontaneous-emission source. Therefore, the unnecessary fast-oscillating terms, which are cancelled after integration along the cavity, do not exist in these new functions.

This paper is organized as follows. In Section II, we start with the scalar wave equation and derive the ASE power spectral density of the radiation field. The wave equation is then solved using the Green's functions of a system of first-order differential operators. The details of constructing the solution using these Green's functions with some corrections to its original form are explained in Section III. In this section, we also relate these new Green's functions to the Green's function proposed by Henry. In Section IV, we apply the formulation in this paper to various surface-emitting DFB lasers and physically interpret the simulation results. Finally, the conclusion and the main results are presented in Section V.

II. Basic Formulation

Let us consider a DFB laser with a second-order index or gain/absorptive grating. The length of the laser cavity is L, which extends from $z = 0$ to $z = L$. Moreover, assume that there is a window in the p- or n-side electrode for extracting the radiated power. Let the electric field be polarized in the lateral direction (along the y axis) and $E(\mathbf{r}, t)$ denote the real-valued

Manuscript received July 22, 2005; revised November 28, 2005.

A. M. Shams-Zadeh-Amiri is with Photonami Corporation, Richmond Hill, ON L4B 1E4, Canada (e-mail: amshams@ieee.org).

W. Li was with Photonami Corporation, Richmond Hill, ON L4B 1E4, Canada. He is now with the Department of Chemistry and Engineering Physics, University of Wisconsin-Platteville, Platteville, WI 53818 USA (e-mail: liw@uwplatt.edu).

H. Wenzel is with the Ferdinand-Braun-Institut für Höchstfrequenztechnik, Berlin 12489, Germany (e-mail: wenzel@FBH-Berlin.de).

X. Li is with the Department of Electrical and Computer Engineering, McMaster University, Hamilton, ON, Canada (e-mail: lixun@mcmaster.ca).

Digital Object Identifier 10.1109/JLT.2006.871035

scalar electric field of the laser. We define the Fourier transform of $E(\mathbf{r},t)$ as follows:

$$\widetilde{E}_\omega(\mathbf{r}) = \frac{1}{\sqrt{2\pi}} \int_{-\infty}^{\infty} E(\mathbf{r},t) e^{-j\omega t} dt \tag{1}$$

where $\mathbf{r} = (x,y,z)$ is the position vector. $\widetilde{E}_\omega(\mathbf{r})$ is the solution of the following inhomogeneous scalar wave equation [13]

$$\nabla^2 \widetilde{E}_\omega(\mathbf{r}) + k_0^2 n_\omega^2(\mathbf{r}) \widetilde{E}_\omega(\mathbf{r}) = \widetilde{F}_\omega(\mathbf{r}) \tag{2}$$

where ∇^2 is the Laplacian operator, $k_0 (= \omega/c)$ is the wavenumber at the optical frequency ω, c is the velocity of light in a vacuum, $n_\omega(\mathbf{r})$ is the complex refractive index of the laser cavity, and $\widetilde{F}_\omega(\mathbf{r})$ is the Langevin force due to the spontaneous emission. One may write the solution of (2) as follows:

$$\widetilde{E}_\omega(\mathbf{r}) = \widetilde{Z}_\omega(z) \Phi_\omega(x,y) + \widetilde{E}_\omega^{r(\mathrm{ASE})}(\mathbf{r}) \tag{3}$$

where $\Phi_\omega(x,y)$ is the eigenmode of the fundamental guided TE mode of the unperturbed cold cavity and satisfies the following eigenvalue equation:

$$\nabla_{xy}^2 \Phi_\omega(x,y) + k_0^2 n_{xy}^2(x,y) \Phi_\omega(x,y) = \beta_\omega^2 \Phi_\omega(x,y). \tag{4}$$

∇_{xy}^2 is the Laplacian operator in the xy plane, i.e., the cross section of the laser cavity; $n_{xy}(x,y)$ is the refractive index of the unperturbed cold cavity; $\beta_\omega = k_0 n_{\mathrm{eff}}$; and n_{eff} is the effective index of the waveguide. $\widetilde{Z}_\omega(z)$ in (3) represents the complex amplitude of the standing wave inside the cavity, which can be written as

$$\widetilde{Z}_\omega(z) = \widetilde{A}_\omega(z) e^{-j\beta_0 z} + \widetilde{B}_\omega(z) e^{j\beta_0 z} \tag{5}$$

where $\beta_0 = 2\pi/\Lambda$, Λ is the period of the grating, and $\widetilde{A}_\omega(z)$ and $\widetilde{B}_\omega(z)$ are the slowly varying complex amplitudes of the forward and backward guided waves, respectively. $\widetilde{E}_\omega^{r(\mathrm{ASE})}(\mathbf{r})$ in (3) is the radiation field due to the ASE. It arises from first-order diffraction. Since the guided waves are responsible for amplification of the spontaneous emission, $\widetilde{E}_\omega^{r(\mathrm{ASE})}(\mathbf{r})$ modifies the coupling coefficients between the amplitudes of the guided waves.

Following Henry [13], we have

$$\widetilde{\mathbf{D}}_\omega^z \left[\widetilde{Z}_\omega(z) \right] = \widetilde{F}_\omega(z) \tag{6}$$

where $\widetilde{\mathbf{D}}_\omega^z$ is a carrier-dependent second-order differential operator with respect to z. The superscript "z" denotes the differentiation variable. $\widetilde{F}_\omega(z)$ is the weighted average of the spontaneous emission coupled to the guided waves with zero mean and is given as follows:

$$\widetilde{F}_\omega(z) = \xi^{-1}(\Phi_\omega) \int_{-\infty}^{\infty} \int_{-\infty}^{\infty} \widetilde{F}_\omega(\mathbf{r}) \Phi_\omega^*(x,y) dx dy \tag{7}$$

where $*$ denotes the complex conjugate, and

$$\xi(\Phi_\omega) = \int_{-\infty}^{\infty} \int_{-\infty}^{\infty} |\Phi_\omega(x,y)|^2 dx dy. \tag{8}$$

Since $\widetilde{F}_\omega(z)$ is the spontaneous emission coupled to the guided waves, it is natural to write

$$\widetilde{F}_\omega(z) = \widetilde{f}_\omega^A(z) e^{-j\beta_0 z} + \widetilde{f}_\omega^B(z) e^{j\beta_0 z}. \tag{9}$$

Note that (9) does not uniquely define $\widetilde{f}_\omega^A(z)$ and $\widetilde{f}_\omega^B(z)$ in terms of $\widetilde{F}_\omega(z)$. However, its special form allows us to have a fair judgment about the statistical properties of $\widetilde{f}_\omega^A(z)$ and $\widetilde{f}_\omega^B(z)$. We will address this issue in Appendix A.

Substituting (3) into (2), one may apply the approaches presented in [14] and [15] and use (7) and (9) to show that, in a general second-order DFB laser with a symmetric grating, $\widetilde{A}_\omega(z)$ and $\widetilde{B}_\omega(z)$ in the presence of spontaneous emission satisfy the following coupled-mode equations:

$$\begin{bmatrix} \mathrm{d}_z \widetilde{A}_\omega(z) \\ -\mathrm{d}_z \widetilde{B}_\omega(z) \end{bmatrix} = \begin{bmatrix} \widetilde{K}_\omega^{11} & \widetilde{K}_\omega^{12} \\ \widetilde{K}_\omega^{21} & \widetilde{K}_\omega^{22} \end{bmatrix} \begin{bmatrix} \widetilde{A}_\omega(z) \\ \widetilde{B}_\omega(z) \end{bmatrix} + \frac{1}{-j2\beta_0} \begin{bmatrix} \widetilde{f}_\omega^A(z) \\ \widetilde{f}_\omega^B(z) \end{bmatrix} \tag{10}$$

where $\mathrm{d}_z \equiv d/dz$, and

$$\widetilde{K}_\omega^{11} = \widetilde{K}_\omega^{22} = \frac{\Gamma g(z)}{2} - \alpha - j\Delta_\omega(z) + \kappa_r \tag{11}$$

$$\widetilde{K}_\omega^{12} = -j \left[\kappa_i + j(\kappa_g + \kappa_r) \right] e^{j2\theta(z)} \tag{12}$$

$$\widetilde{K}_\omega^{21} = -j \left[\kappa_i + j(\kappa_g + \kappa_r) \right] e^{-j2\theta(z)} \tag{13}$$

where κ_i and κ_g are the coupling coefficients due to in-plane feedback (second-order diffraction) resulting from index and gain/absorption perturbations within the laser cavity, respectively. κ_r represents the reaction of the radiation field excited by the guided waves back on themselves due to the first-order diffraction. $\theta(z)$ is the phase of the first-order spatial harmonic of the grating. In this paper, we assume that the index and gain/absorption perturbations are obtained by the same grating. For a gain perturbation, $\theta(z)$ is defined by (A9). A similar relation is assumed for an index perturbation. The dependence of θ on z allows us to include the phase-shifted DFB lasers in the model as well. For a DFB laser with discrete phase shifts, $\theta(z)$ is a step function of z. The factor 2 in front of $\theta(z)$ results from second-order diffraction or two consecutive first-order diffractions, Γ is the confinement factor, $g(z)$ is the intensity material gain, α is the internal loss, and $\Delta_\omega(z)$ is the measure of detuning given as

$$\begin{aligned} \Delta_\omega(z) &= \beta_\omega - \alpha_H \Gamma \frac{g(z)}{2} - \beta_0 \\ &= \frac{\omega - \omega_B}{v_g} - \alpha_H \Gamma \frac{g(z)}{2} \end{aligned} \tag{14}$$

where α_H is the linewidth enhancement factor [16], ω_B is the Bragg frequency, and v_g is the group velocity.

The main goal in this paper is to obtain the ASE spectrum of the radiation field emitted from the surface of the laser. To

this end, in the absence of spontaneous emission and using (10)–(13), one may write

$$\begin{aligned}\mathrm{d}_z&\left[\left|\widetilde{A}_\omega(z)\right|^2-\left|\widetilde{B}_\omega(z)\right|^2\right]\\&=[\Gamma g(z)-2\alpha]\left[\left|\widetilde{A}_\omega(z)\right|^2+\left|\widetilde{B}_\omega(z)\right|^2\right]\\&\quad+2\mathrm{Re}(\kappa_r)\left|e^{-j\theta(z)}\widetilde{A}_\omega(z)+e^{j\theta(z)}\widetilde{B}_\omega(z)\right|^2\\&\quad+2\kappa_g\left[e^{-j2\theta(z)}\widetilde{A}_\omega(z)\widetilde{B}^*_\omega(z)+e^{j2\theta(z)}\widetilde{A}^*_\omega(z)\widetilde{B}_\omega(z)\right]\end{aligned}\tag{15}$$

where "Re" stands for the real part. Equation (15), which is the power exchange relation inside the cavity, states that the radiation power density is proportional to $|e^{-j\theta(z)}\widetilde{A}_\omega(z)+e^{j\theta(z)}\widetilde{B}_\omega(z)|^2$. On the other hand, due to normal emission ($\partial/\partial z\approx 0$), the radiating electric and magnetic fields obey the plane-wave relation, and the magnetic field has only a component along the z-axis. From Maxwell's equations, it follows that

$$\widetilde{H}^{r(\mathrm{ASE})}_\omega(z)=\pm\eta^{-1}\widetilde{E}^{r(\mathrm{ASE})}_\omega(z)\tag{16}$$

where $\widetilde{E}^{r(\mathrm{ASE})}_\omega(z)$ and $\widetilde{H}^{r(\mathrm{ASE})}_\omega(z)$ are the longitudinal profiles of the radiating electric and magnetic fields, respectively, and $\eta=(\mu_0/\varepsilon)^{1/2}$ is the so-called intrinsic impedance of the medium. μ_0 and ε are the permeability of vacuum and permittivity of the medium, respectively. From (15) and (16), it follows that

$$\widetilde{E}^{r(\mathrm{ASE})}_\omega(z)\sim\widetilde{A}_\omega(z)e^{-j\theta(z)}+\widetilde{B}_\omega(z)e^{j\theta(z)}.\tag{17}$$

Let $E^{r(\mathrm{ASE})}(z,t)$ and $\widetilde{S}^{r(\mathrm{ASE})}_\omega(z)$ be the z-dependent part of the real-valued radiating electric field in the time domain due to ASE and the z-dependent power spectral density of the radiation field, respectively. Using (16) and the fact that the laser field in the presence of the spontaneous emission is a stationary random process, according to the Wiener–Khintchine theorem, the power spectral density of the radiation field is proportional to the Fourier transform of its autocorrelation, i.e.,

$$\widetilde{S}^{r(\mathrm{ASE})}_\omega(z)\sim\int_{-\infty}^{\infty}\left\langle E^{r(\mathrm{ASE})}(z,0+\tau)E^{r(\mathrm{ASE})}(z,0)\right\rangle e^{-j\omega\tau}d\tau\tag{18}$$

where $\langle\cdot\rangle$ denotes the ensemble average. In (18), we have set $t=0$, which is justified assuming the stationary character of the laser field and the fact that its statistical properties are independent of the time origin. Substituting $E^{r(\mathrm{ASE})}(z,\cdot)$ by its Fourier transform and the fact that the Fourier transform of a real function possesses conjugate symmetry, i.e., $\widetilde{E}^{r(\mathrm{ASE})}_{-\omega'}(z)=\widetilde{E}^{r(\mathrm{ASE})*}_{\omega'}(z)$, we get

$$\widetilde{S}^{r(\mathrm{ASE})}_\omega(z)\sim\int_{-\infty}^{\infty}\left\langle\widetilde{E}^{r(\mathrm{ASE})}_\omega(z)\widetilde{E}^{r(\mathrm{ASE})*}_{\omega'}(z)\right\rangle d\omega'.\tag{19}$$

Let $\widetilde{S}^{r(\mathrm{ASE})}_\omega$ be the power spectrum of the radiation field due to the ASE. $\widetilde{S}^{r(\mathrm{ASE})}_\omega$ can be obtained by integrating $\widetilde{S}^{r(\mathrm{ASE})}_\omega(z)$ along the window from which the radiated power is extracted, i.e.,

$$\widetilde{S}^{r(\mathrm{ASE})}_\omega=\int_{\mathrm{window}}\widetilde{S}^{r(\mathrm{ASE})}_\omega(z)dz.\tag{20}$$

Equations (17), (19), and (20) are the main equations for obtaining the ASE spectrum of the radiation field in a surface-emitting DFB laser with a second-order grating. To calculate $\widetilde{S}^{r(\mathrm{ASE})}_\omega(z)$ using (17) and (19), one needs to obtain the autocorrelation and cross correlation of $\widetilde{A}_\omega(z)$ and $\widetilde{B}_\omega(z)$. To this end, one may obtain $\widetilde{A}_\omega(z)$ and $\widetilde{B}_\omega(z)$ in terms of the spontaneous-emission source. We use the Green's function method for this purpose. The details of this method will be discussed in the next section.

III. Green's Function Formulation

To obtain $\widetilde{A}_\omega(z)$ and $\widetilde{B}_\omega(z)$ in terms of the spontaneous emission, one may adopt two different but equivalent approaches. In the first approach, which was originally proposed by Henry [13], one may solve (6) and obtain $\widetilde{Z}_\omega(z)$ in terms of $\widetilde{F}_\omega(z)$ as follows:

$$\widetilde{Z}_\omega(z)=\int_0^L\widetilde{G}_\omega(z,z')\widetilde{F}_\omega(z')dz'\tag{21}$$

where the Green's function $\widetilde{G}_\omega(z,z')$ satisfies the following second-order differential equation:

$$\widetilde{\mathbf{D}}^z_\omega\lfloor\widetilde{G}_\omega(z,z')\rfloor=\delta(z-z')\tag{22}$$

subject to the boundary conditions at $z=0$ and $z=L$. $\delta(\cdot)$ is the Dirac delta function. $\widetilde{G}_\omega(z,z')$ can be obtained in terms of the solution of homogenous differential equation obtained from (22) by setting its right-hand side equal to 0. On the other hand, the solution of the resulting homogenous equation is in the form of (5). Thus, $\widetilde{Z}_\omega(z)$ in the presence of $\widetilde{F}_\omega(z)$ is in the same form as given in (5); therefore, one may obtain $\widetilde{A}_\omega(z)$ and $\widetilde{B}_\omega(z)$ in terms of $\widetilde{F}_\omega(z)$. Moreover, one may use (9) to simplify the final result by canceling the fast-oscillating terms under the integral sign. The unnecessary terms resulting from this approach make the algebraic manipulation lengthy.

Recently, the direct solution of (10) and obtaining $\widetilde{A}_\omega(z)$ and $\widetilde{B}_\omega(z)$ in terms of $\widetilde{f}^A_\omega(z)$ and $\widetilde{f}^B_\omega(z)$ by defining suitable vector Green's functions have been reported in [12]. The distinguishing feature in this approach is the use of slowly varying functions of z instead of dealing with the general form of $\widetilde{Z}_\omega(z)$. The essence of this approach is based on rewriting (10) as follows:

$$\widetilde{\mathbf{H}}^z_\omega\widetilde{\Psi}_\omega(z)=\widetilde{\mathbf{F}}_\omega(z)\tag{23}$$

where

$$\widetilde{\mathbf{H}}^z_\omega=\begin{bmatrix}\mathrm{d}_z-\widetilde{K}^{11}_\omega & -\widetilde{K}^{12}_\omega\\ -\widetilde{K}^{21}_\omega & -\mathrm{d}_z-\widetilde{K}^{22}_\omega\end{bmatrix}\tag{24}$$

the superscript "z" indicates the variable of differentiation

$$\widetilde{\Psi}_\omega(z) = \begin{bmatrix} \widetilde{A}_\omega(z) \\ \widetilde{B}_\omega(z) \end{bmatrix} \tag{25}$$

and

$$\widetilde{\mathbf{F}}_\omega(z) = \frac{1}{-j2\beta_0} \begin{bmatrix} \widetilde{f}^A_\omega(z) \\ \widetilde{f}^B_\omega(z) \end{bmatrix}. \tag{26}$$

A symmetric bilinear form [17, pp. 365–367] in the space of $\widetilde{\Psi}_\omega(z)$ is defined as follows:

$$\left\langle \widetilde{\Psi}^{(1)}_\omega, \widetilde{\Psi}^{(2)}_\omega \right\rangle = \int_0^L \left[\widetilde{A}^{(1)}_\omega(z)\widetilde{B}^{(2)}_\omega(z) + \widetilde{B}^{(1)}_\omega(z)\widetilde{A}^{(2)}_\omega(z) \right] dz \tag{27}$$

where

$$\widetilde{\Psi}^{(i)}_\omega(z) = \begin{bmatrix} \widetilde{A}^{(i)}_\omega(z) \\ \widetilde{B}^{(i)}_\omega(z) \end{bmatrix}, \qquad i = 1, 2. \tag{28}$$

$\widetilde{\mathbf{H}}^z_\omega$ in the sense of the bilinear form defined in (27) is symmetric, i.e.,

$$\left\langle \widetilde{\mathbf{H}}^z_\omega \widetilde{\Psi}^{(1)}_\omega, \widetilde{\Psi}^{(2)}_\omega \right\rangle - \left\langle \widetilde{\Psi}^{(1)}_\omega, \widetilde{\mathbf{H}}^z_\omega \widetilde{\Psi}^{(2)}_\omega \right\rangle = 0. \tag{29}$$

Equation (29) follows from the fact that $\widetilde{A}^{(i)}_\omega(z)$ and $\widetilde{B}^{(i)}_\omega(z)$ satisfy the same boundary conditions at $z = 0$ and $z = L$, i.e., $\widetilde{A}^{(i)}_\omega(0) = r_0\widetilde{B}^{(i)}_\omega(0)$ and $\widetilde{B}^{(i)}_\omega(L) = r_L\widetilde{A}^{(i)}_\omega(L)$. It should be emphasized that for the case of nonuniform carrier distribution inside the cavity, by dividing the laser cavity into sufficiently large number of sections, one may assume that the carrier distribution within each section is uniform. Therefore, $g(z)$ can be approximated by a step function, and (29) is still valid within this approximation.

The solutions for $\widetilde{A}_\omega(z)$ and $\widetilde{B}_\omega(z)$ can be obtained by introducing the following vector Green's functions:

$$\widetilde{\mathbf{G}}_{i,\omega}(z, z') = \begin{bmatrix} \widetilde{g}^A_{i,\omega}(z, z') \\ \widetilde{g}^B_{i,\omega}(z, z') \end{bmatrix}, \qquad i = 1, 2 \tag{30}$$

such that

$$\widetilde{\mathbf{H}}^z_\omega \widetilde{\mathbf{G}}_{1,\omega}(z, z') = \begin{bmatrix} 0 \\ \delta(z - z') \end{bmatrix} \tag{31}$$

and

$$\widetilde{\mathbf{H}}^z_\omega \widetilde{\mathbf{G}}_{2,\omega}(z, z') = \begin{bmatrix} \delta(z - z') \\ 0 \end{bmatrix} \tag{32}$$

subject to the boundary conditions at $z = 0$ and $z = L$, i.e., $\widetilde{g}^A_{i,\omega}(0, z') = r_0\widetilde{g}^B_{i,\omega}(0, z')$, and $\widetilde{g}^B_{i,\omega}(L, z') = r_L\widetilde{g}^A_{i,\omega}(L, z')$. In fact, using (25), (27), and (31), one may write

$$\widetilde{A}_\omega(z') = \left\langle \widetilde{\mathbf{H}}^z_\omega \widetilde{\mathbf{G}}_{1,\omega}(z, z'), \widetilde{\Psi}_\omega(z) \right\rangle. \tag{33}$$

In view of the symmetry of $\widetilde{\mathbf{H}}^z_\omega$, (33) can be written as

$$\widetilde{A}_\omega(z') = \left\langle \widetilde{\mathbf{G}}_{1,\omega}(z, z'), \widetilde{\mathbf{F}}_\omega(z) \right\rangle \tag{34}$$

where we have used (23). Following the same procedure and replacing $\widetilde{\mathbf{G}}_{1,\omega}(z, z')$ by $\widetilde{\mathbf{G}}_{2,\omega}(z, z')$ in (34), one may obtain $\widetilde{B}_\omega(z')$. Changing the roles of z and z' in (34), we can write the solution for $\widetilde{\Psi}_\omega(z)$ as follows:

$$\widetilde{\Psi}_\omega(z) = \begin{bmatrix} \left\langle \widetilde{\mathbf{G}}_{1,\omega}(z', z), \widetilde{\mathbf{F}}_\omega(z') \right\rangle \\ \left\langle \widetilde{\mathbf{G}}_{2,\omega}(z', z), \widetilde{\mathbf{F}}_\omega(z') \right\rangle \end{bmatrix} \tag{35}$$

where z' is the variable of integration.

It should be noted that due to the presence of first-order differential operator and the Dirac delta function in (31) and (32), $\widetilde{g}^B_{1,\omega}(z, z')$ and $\widetilde{g}^A_{2,\omega}(z, z')$ are discontinuous at $z = z'$. Therefore, the Green's functions $\widetilde{\mathbf{G}}_{i,\omega}(z, z')$, $i = 1, 2$, are not symmetric with respect to their arguments, and the roles of z and z' as the arguments of the Green's functions in (35) cannot be changed.

The vector Green's functions $\widetilde{\mathbf{G}}_{1,\omega}(z, z')$ and $\widetilde{\mathbf{G}}_{2,\omega}(z, z')$ have some interesting properties. In fact, using the symmetry of $\widetilde{\mathbf{H}}^z_\omega$, we have

$$\begin{aligned} &\left\langle \widetilde{\mathbf{H}}^z_\omega \widetilde{\mathbf{G}}_{i,\omega}(z, z_1), \widetilde{\mathbf{G}}_{j,\omega}(z, z_2) \right\rangle \\ &\quad = \left\langle \widetilde{\mathbf{G}}_{i,\omega}(z, z_1), \widetilde{\mathbf{H}}^z_\omega \widetilde{\mathbf{G}}_{j,\omega}(z, z_2) \right\rangle, \qquad i, j = 1, 2. \end{aligned} \tag{36}$$

Let $\widetilde{\mathbf{G}}_\omega(z_1, z_2)$ be a 2×2 matrix such that its first and second columns are formed by entries of the column vectors $\widetilde{\mathbf{G}}_{1,\omega}(z_1, z_2)$ and $\widetilde{\mathbf{G}}_{2,\omega}(z_1, z_2)$, respectively. Using (36), one may write

$$\widetilde{\mathbf{G}}_\omega(z_1, z_2) = \widetilde{\mathbf{G}}^{\mathrm{T}}_\omega(z_2, z_1) \tag{37}$$

where "T" stands for the transpose. It is interesting to note that the Green's function $\widetilde{G}_\omega(z, z')$ defined by (22) can be obtained using $\widetilde{\mathbf{G}}_\omega(z, z')$ as follows:

$$\widetilde{G}_\omega(z, z') = \frac{1}{-j2\beta_0} [e^{-j\beta_0 z'} \quad e^{j\beta_0 z'}] \widetilde{\mathbf{G}}_\omega(z', z) \begin{bmatrix} e^{-j\beta_0 z} \\ e^{j\beta_0 z} \end{bmatrix}. \tag{38}$$

Using (37) and (38), one may obtain the well-known reciprocity formula of $\widetilde{G}_\omega(z, z')$, i.e.,

$$\widetilde{G}_\omega(z, z') = \widetilde{G}_\omega(z', z). \tag{39}$$

Using the Green's function formulation in (17) and (19) and the materials presented in Appendix A, the reader may verify that the z-dependent power spectral density of the radiation field can be obtained as follows:

$$\begin{aligned} &\widetilde{S}^{r(\mathrm{ASE})}_\omega(z) \\ &\quad \sim \left(4\beta_0^2\right)^{-1} \int_0^L \left|\widetilde{g}^A_\omega(z', z)\right|^2 \times 2D_{\widetilde{f}^B \widetilde{f}^{B*}}(z')dz' \\ &\qquad + \left(4\beta_0^2\right)^{-1} \int_0^L \left|\widetilde{g}^B_\omega(z', z)\right|^2 \times 2D_{\widetilde{f}^A \widetilde{f}^{A*}}(z')dz' + \left(4\beta_0^2\right)^{-1} \\ &\qquad \cdot \int_0^L 2\mathrm{Re}\left[\widetilde{g}^A_\omega(z', z)\widetilde{g}^{B*}_\omega(z', z) \times 2D_{\widetilde{f}^B \widetilde{f}^{A*}}(z')\right] dz' \end{aligned} \tag{40}$$

where

$$\widetilde{g}_{\omega}^{A,B}(z',z) = \widetilde{g}_{1,\omega}^{A,B}(z',z)e^{-j\theta(z)} + \widetilde{g}_{2,\omega}^{A,B}(z',z)e^{j\theta(z)}. \quad (41)$$

$\widetilde{g}_{1,\omega}^{A,B}(z',z)$ and $\widetilde{g}_{2,\omega}^{A,B}(z',z)$ can be obtained from $\widetilde{\mathbf{G}}_{1,\omega}(z,z')$ and $\widetilde{\mathbf{G}}_{2,\omega}(z,z')$ and using (37). The details of the derivation of the explicit expressions for $\widetilde{\mathbf{G}}_{1,\omega}(z,z')$ and $\widetilde{\mathbf{G}}_{2,\omega}(z,z')$ are given in Appendix B. $2D_{\widetilde{f}^A\widetilde{f}^{A*}}$, $2D_{\widetilde{f}^B\widetilde{f}^{B*}}$, and $2D_{\widetilde{f}^B\widetilde{f}^{A*}}$ are the diffusion coefficients of the spontaneous emission, which are given in Appendix A.

Equations (20) and (40) are the main results of this paper. They give the ASE spectrum of the radiation field in terms of the carrier-dependent Green's functions and the diffusion coefficients of the spontaneous emission. Equation (40) is valid both in the below- and above-threshold regimes. However, its applicability in the above-threshold regime requires the knowledge of the exact carrier distribution within the cavity. To obtain the carrier distribution in the above-threshold regime, the nonlinear interaction of the optical field with the carrier density should be formulated by the multimode rate equations. In this paper, we only use (40) in the below-threshold regime in which the carrier distribution within the cavity can be considered uniform.

For the sake of completeness and comparison, the spectral density of ASE from the left facet is given as follows:

$$\widetilde{S}_{\omega}^{\text{left}} \sim \left(1-|r_0|^2\right)\left(4\beta_0^2\right)^{-1} \times\left(\int_0^L \left|\widetilde{g}_{2,\omega}^{A}(z',0)\right|^2 2D_{\widetilde{f}^B\widetilde{f}^{B*}}(z')dz' + \int_0^L \left|\widetilde{g}_{2,\omega}^{B}(z',0)\right|^2 2D_{\widetilde{f}^A\widetilde{f}^{A*}}(z')dz' + \int_0^L 2\text{Re}\left[\widetilde{g}_{2,\omega}^{A}(z',0)\widetilde{g}_{2,\omega}^{B*}(z',0)2D_{\widetilde{f}^B\widetilde{f}^{A*}}(z')\right]dz'\right). \quad (42)$$

The ASE spectrum from the right facet can be obtained from (42) by replacing r_0 and $\widetilde{g}_{2,\omega}^{A,B}(z',0)$ with r_L and $\widetilde{g}_{1,\omega}^{A,B}(z',L)$, respectively.

IV. Simulation Results

In this section, we apply the formulation given in this paper to obtain the below-threshold ASE spectrum of the radiation field in three different surface-emitting DFB lasers. The fixed parameters of these lasers are given in Table I. To show the intrinsic characteristics of these lasers, we assume that their facets are antireflection (AR) coated. In all cases, we consider buried-heterostructure (BH) lasers with a window of 100-μm long, which opens in the p-side electrode. The center of the window is aligned with the center of the cavity. Note that the window opening can also be extended throughout the length of the cavity. All spectra are calculated at 95% of the threshold gains.

TABLE I
Parameters Used in the Below-Threshold Analysis of Second-Order DFB Lasers

Parameters	Values
Cavity length (L)	300 μm
Index-coupling coefficient ($\|\kappa_i\|$)	100 cm^{-1}
Radiation coupling coefficient (κ_r)	-5+j4 cm^{-1}
Effective index of the cold cavity (n_{eff})	3.23
Linewidth enhancement factor (α_H)	3.0
Internal loss (α)	10 cm^{-1}
Grating period (Λ)	480 nm

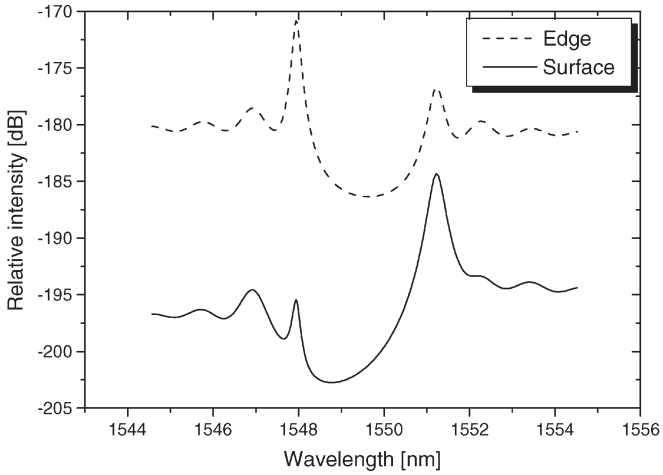

Fig. 1. Below-threshold ASE spectra of a DFB laser with a second-order index grating and 25% duty cycle.

In the first example, we consider a DFB laser with a second-order index grating and duty cycle of 25%. The duty cycle is defined as the ratio of the width of the grating tooth with the higher refractive index to the grating period. For this laser, κ_i is positive. Therefore, based on the assumed value of $|\kappa_i|$ in Table I, we have $\kappa_i = 100$ cm^{-1}. Since $\text{Re}(\kappa_r) < 0$, the grating is antiphase, which means that the main mode will be at the shorter wavelength side of the stopband: the so-called $+1$ mode (positive detuning). The below-threshold power spectra from the surface and edge of this laser are plotted in Fig. 1. Using the ASE spectrum from the edge, one may see that the intensity of $+1$ mode is higher than the intensity of the mode at the longer wavelength side of the stopband: the so-called -1 mode (negative detuning). The reason is that the $+1$ mode sees more gain in an antiphase grating, and its intensity is higher than that of the -1 mode. However, as illustrated in Fig. 1, the ASE spectrum from the surface reveals that the intensity of the -1 mode is higher than the intensity of the $+1$ mode. This behavior can be explained by noting that, in a DFB laser with a second-order index grating, the guided waves forming the main mode interfere destructively, and its near-field radiation pattern has a minimum at the center of the cavity. On the other hand, formation of the first side mode is due to constructive interference between the guided waves forming that mode, and its near-field radiation pattern has a maximum at the center of the cavity [3]. Compared to the edge-emitted power spectrum, this characteristic feature of DFB lasers with a second-order

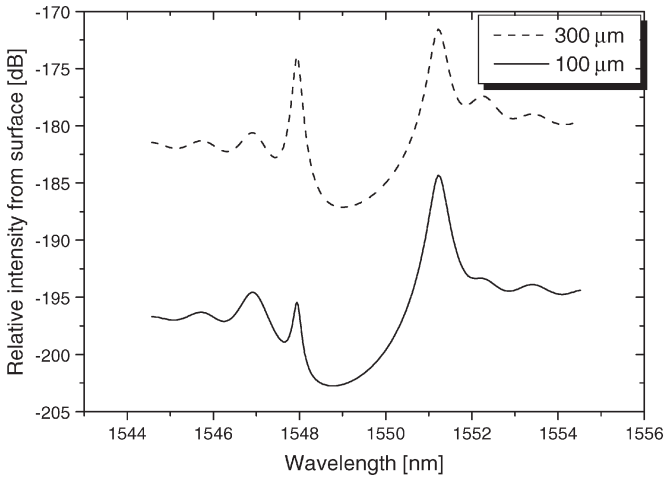

Fig. 2. Effect of the window size on the ASE spectrum of the radiation field. The window sizes are chosen as 100 and 300 μm, respectively.

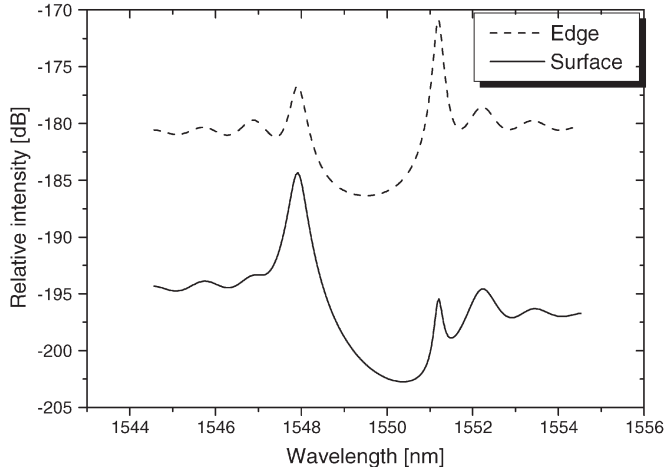

Fig. 3. Below-threshold ASE spectra of a DFB laser with a second-order index grating and 75% duty cycle.

index grating reduces the relative intensity between the main mode and first side mode emitted from the surface. Therefore, in a surface-emitting DFB laser with a second-order index grating, one may expect that the SMSR of the surface-emitted power is less than the SMSR of the power emitted from the edge.

Due to the near-field radiation patterns of the main mode and first side mode, one may expect that increasing the window size reduces the relative intensity between these two modes of the radiation field. This fact is illustrated in Fig. 2.

By increasing the duty cycle of the grating to more than 50%, e.g., 75%, the sign of κ_i changes; since the sign of $\mathrm{Re}(\kappa_r)$ remains unchanged, we deal with an inphase grating. A DFB laser with such grating favors the -1 mode. However, the formation of the main mode and first side mode is still based on destructive and constructive interference between the guided waves. Therefore, based on the principles explained earlier, one may expect that the spectra from the surface and edge can be obtained from those with duty cycles of 25% and by switching the intensities of the $+1$ and -1 modes, respectively, as depicted in Fig. 3.

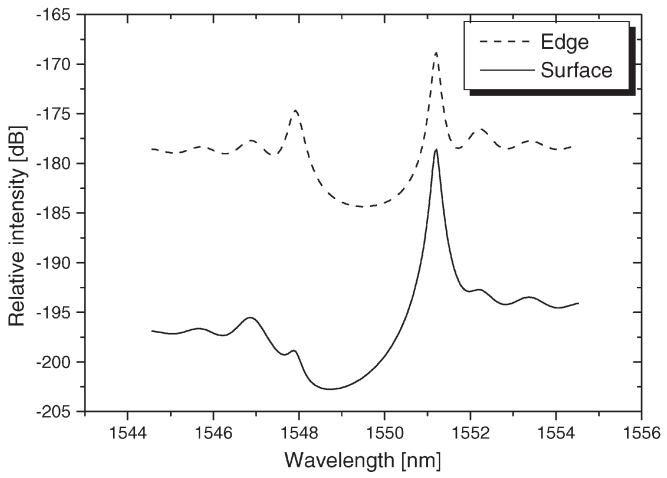

Fig. 4. Below-threshold ASE spectra of a DFB laser with a second-order gain grating such that $\kappa_g + \mathrm{Re}(\kappa_r) > 0$.

It should be noted that the power spectra in Figs. 1 and 3 correspond to two different DFB lasers with the same value of $\mathrm{Re}(\kappa_r)$, whereas their κ_i values are of the same magnitude but opposite signs. Therefore, at threshold, the so-called standing wave factors [18] of the main modes of these two lasers are almost the same and the same holds true for their first side modes. On the other hand, the signs of the κ_i values of these two DFB lasers are opposite of each other. Then, according to Beats *et al.* [18, eq. (13)], the detunings of the main mode and first side mode in the first laser are almost negative of the corresponding detunings in the second laser. Therefore, with respect the Bragg wavelength, the wavelengths of the main mode and first side mode in the first lasers are almost the mirror images of the corresponding wavelengths of those modes in the second laser. The fact that power spectra shown in Figs. 1 and 3 are almost the mirror images of each other is consistent with the above argument.

Theoretical investigation of second-order resonant gratings with gain or absorption has been considered in [15] and [19]. As pointed out in [9] and [19], the main mode of a DFB laser with a second-order gain grating may have a near-field radiation pattern with a peak at the center of the cavity. This mode is formed by constructive interference between the guided waves inside the cavity. The overlap between the intensity of the main mode and the gain grating dominates the radiation loss, and the mode selection is based on this overlap mechanism. The condition for excitation of such mode is $\kappa_g > -\mathrm{Re}(\kappa_r)$, and it may happen if the duty cycle of the grating is less than 50%. For such a DFB laser, let $\kappa_i = 100\ \mathrm{cm}^{-1}$, $\kappa_g = 10\ \mathrm{cm}^{-1}$, and $\kappa_r = -5 + j4\ \mathrm{cm}^{-1}$. With these parameters, the grating is in-phase, and -1 mode is the main mode. However, since $\kappa_g + \mathrm{Re}(\kappa_r) > 0$, the main mode has a near-field radiation pattern with a peak at the center of the cavity. Due to this feature, the relative intensity between the main mode and first side mode emitted from the surface is more than that from the edge. This fact is illustrated in Fig. 4.

In DFB lasers with a second-order grating in the active region, it is possible to adjust the grating duty cycle to have a negative κ_g. In fact, for duty cycles more than 50%, κ_i

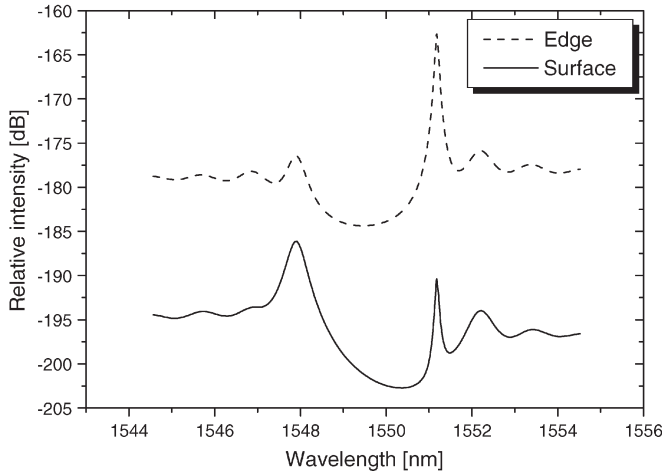

Fig. 5. Below-threshold ASE spectra of a DFB laser with a second-order gain grating and duty cycle of 75%.

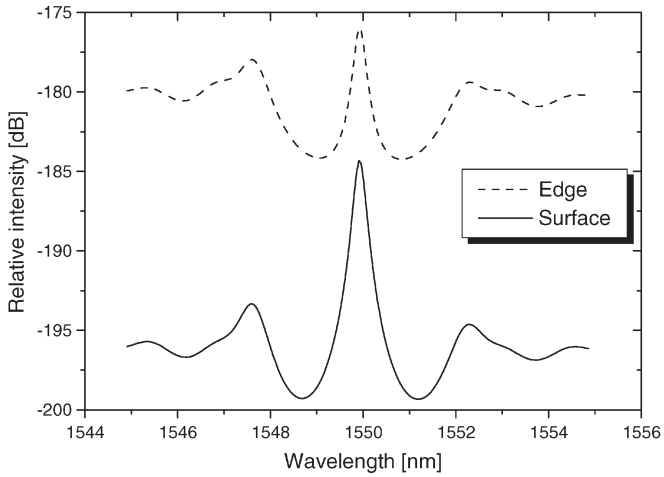

Fig. 6. Below-threshold ASE spectra of a quarter-wave phase-shifted DFB laser with a second-order index grating and duty cycle of 25%.

and κ_g are negative. This is the main difference between first- and second-order gain gratings. Moreover, since $\mathrm{Re}(\kappa_r) < 0$ in second-order gratings etched into the active part, it follows that $\kappa_g + \mathrm{Re}(\kappa_r) < 0$ for duty cycles more than 50%; therefore, the main mode is formed by destructive interference between the guided waves inside the cavity. In this case, in addition to the radiation loss, the overlap between the intensity pattern and the gain grating is in favor of the main mode and enhances the mode selectivity based on the radiation loss. Therefore, one may expect that the main mode is strongly favored. These facts were experimentally verified in a DFB laser made by a truncated quantum well second-order grating with an SMSR over 64 dB [20]. In Fig. 5, the below-threshold power spectra from the surface and edge of a second-order DFB laser with a gain grating of 75% duty cycle are illustrated. The coupling coefficients are $\kappa_i = -100$ cm^{-1}, $\kappa_g = -5$ cm^{-1}, and $\kappa_r = -5 + j4$ cm^{-1}. In this case, the grating is in-phase, and the -1 mode is the main mode. This mode is formed by destructive interference between the guided waves. Therefore, if one measures the ASE spectrum of the radiation field and compares it with the ASE spectrum of the edge-emitted power, one may expect that the relative intensity between the main mode and first side mode emitted from the surface is less than that from the edge. This fact is illustrated in Fig. 5.

Finally, in the last example, we consider a quarter-wave phase-shifted DFB laser with a second-order index grating. This design was first proposed by Kinoshita [4] to avoid the inherent problem of second-order DFB lasers with an index grating. In this structure, the mode selectivity is mainly due to the quarter-wave phase shift. The below-threshold ASE spectra from the surface and the edge of such structure with a grating of 25% duty cycle are depicted in Fig. 6. These spectra are calculated based on $\kappa_i = 100$ cm^{-1} and $\kappa_r = -5 + j4$ cm^{-1}. Interestingly enough, if we compare these spectra, we see that the relative intensities between the main mode, the so-called 0 mode (almost zero detuning) and ± 1 modes emitted from the surface are more than those from the edge. The same result is obtained for duty cycles of more than 50%, e.g., 75%, which is not plotted here. Therefore, these lasers are good candidates for surface-emitting DFB lasers both in terms of the radiation mode profile and the spectrum.

V. Conclusion

In this paper, we have formulated the ASE spectrum of the radiation field in surface-emitting DFB lasers with a second-order grating. We have shown that, in comparison with the edge-emitted power spectrum, the interference between the counter-propagating guided waves inside the cavity dramatically changes the relative intensities between the main and other side modes of the radiation field. This feature makes the SMSR of the radiation power less than the SMSR of the power emitted from the edge in a second-order DFB laser with a nonphase-shifted index grating. Increasing the window size enhances the SMSR of the surface-emitted power. On the other hand, it is possible to design a DFB laser with a second-order grating in the active region such that the main mode is excited by the constructive interference between the counter-propagating guided waves inside the cavity. In this case, compared to the edge-emitted power spectrum, the relative intensity between the main mode and first side mode of the radiation field enhances.

A quarter-wave phase-shifted DFB laser with a second-order index grating has the salient features that make this laser an appropriate surface-emitting design in terms of the radiation field pattern and the spectrum.

Appendix A

In semiconductor lasers, we are confronted with the spontaneous emission, which is a stationary Gaussian process. It has a power spectrum that is essentially flat within the linewidth of the gain spectrum in which the main mode and other important side modes of the laser exist. On the other hand, the laser field of a DFB laser like all other lasers is ASE, which is highly filtered. This means that the spontaneous emission outside the linewidth of the gain spectrum cannot be amplified and is highly rejected through the filtering action of the laser cavity. Consequently, as far as the laser field and the effect of the noise power

on it are concerned, it makes little difference precisely how the spontaneous-emission spectrum approaches zero outside the linewidth of the gain spectrum. Thus, we assume that the spontaneous-emission spectrum is flat for all wavelengths and acts as a white noise. According to the Wiener–Khintchine theorem, the autocorrelation of a white noise is expressed in terms of the Dirac delta function. Moreover, from [13], it also has a negligible spatial correlation. Thus

$$\langle F(\mathbf{r},t)F(\mathbf{r}',t')\rangle = 2D_{FF}\delta(\mathbf{r}-\mathbf{r}')\delta(t-t') \tag{A1}$$

where $F(\mathbf{r},t)$ is the real-valued time-domain Langevin force. The so-called diffusion coefficient $2D_{FF}$ is independent of time. Let $\widetilde{F}_\omega(\mathbf{r})$ be the Fourier transform of $F(\mathbf{r},t)$ defined by a transform relation similar to (1). From the stationary character of $F(\mathbf{r},t)$ and the fact that $2D_{FF}$ is independent of time, it can be shown that

$$\begin{aligned}\left\langle \widetilde{F}_\omega(\mathbf{r})\widetilde{F}^*_{\omega'}(\mathbf{r}')\right\rangle &= \left\langle \widetilde{F}^*_\omega(\mathbf{r})\widetilde{F}_{\omega'}(\mathbf{r}')\right\rangle \\ &= 2D_{FF}\delta(\mathbf{r}-\mathbf{r}')\delta(\omega-\omega').\end{aligned} \tag{A2}$$

It should be emphasized that the equality of the diffusion coefficients in the time and frequency domains is the direct consequence of defining a symmetric Fourier transform. More precisely, the diffusion coefficient in the frequency domain depends on the definition of the Fourier transform.

From [13] and by equating the noise power obtained from the principles of statistical mechanics and electromagnetic theory in the SI units, we get

$$2D_{FF} = \frac{2\hbar\omega^3 n(\mathbf{r})g(\mathbf{r})n_{\rm sp}}{\varepsilon_0 c^3} \tag{A3}$$

where $\hbar$ $(=h/2\pi)$ is the reduced Planck constant, $n(\mathbf{r})$ is the refractive index of the active region, $g(\mathbf{r})$ is the intensity gain, $n_{\rm sp}$ is the so-called inversion factor, ε_0 is the permittivity of vacuum, and c is the velocity of light in vacuum.

Strictly speaking, as indicated by (A3), the diffusion coefficient is frequency dependent, and (A1) cannot be derived from (A2) and (A3). However, as mentioned earlier, since only the spontaneous-emission power within the linewidth of the gain spectrum is important, we assume that the spontaneous-emission spectrum is flat for all wavelengths. Without loss of generality, one may consider a flat gain model and set $\omega=\omega_0$ in (A3), where ω_0 is a frequency very close to the lasing frequency.

From (7), (A2), and (A3), it follows that

$$\left\langle \widetilde{F}_\omega(z)\widetilde{F}^*_{\omega'}(z')\right\rangle = \frac{2\hbar\omega_0^3 n(z)\Gamma g(z)n_{\rm sp}}{\varepsilon_0 c^3\xi(\Phi_\omega)}\delta(z-z')\delta(\omega-\omega') \tag{A4}$$

where Γ is the confinement factor, and $\xi(\Phi_\omega)$ is given by (8).

On the other hand, using (9) in an index grating, one may show that

$$\left\langle \widetilde{f}^A_\omega(z)\widetilde{f}^{A*}_{\omega'}(z')\right\rangle + \left\langle \widetilde{f}^B_\omega(z)\widetilde{f}^{B*}_{\omega'}(z')\right\rangle = \left\langle \widetilde{F}_\omega(z)\widetilde{F}^*_{\omega'}(z')\right\rangle \tag{A5}$$

and

$$\left\langle \widetilde{f}^A_\omega(z)\widetilde{f}^{B*}_{\omega'}(z')\right\rangle = \left\langle \widetilde{f}^B_\omega(z)\widetilde{f}^{A*}_{\omega'}(z')\right\rangle = 0. \tag{A6}$$

For a spontaneously emitted photon, the probability of traveling to the left and to the right is the same. Therefore, we have

$$\left\langle \widetilde{f}^i_\omega(z)\widetilde{f}^{i*}_{\omega'}(z')\right\rangle = 2D_{\widetilde{f}^i\widetilde{f}^{i*}}\delta(\omega-\omega')\delta(z-z') \tag{A7}$$

where $i=A$ or B, and

$$2D_{\widetilde{f}^A\widetilde{f}^{A*}} = 2D_{\widetilde{f}^B\widetilde{f}^{B*}} = \frac{\hbar\omega_0^3 n(z)\Gamma g(z)n_{\rm sp}}{\varepsilon_0 c^3\xi(\Phi_\omega)}. \tag{A8}$$

For a gain-coupled DFB laser, we have

$$g(z) = g_{\rm av}(z) + \sum_{n\neq 0} g_n(z)e^{-jn\left[\frac{2\pi}{\Lambda}z-\theta(z)\right]} \tag{A9}$$

where Λ and $\theta(z)$ are the period and the phase of the grating, respectively. It should be noted that (A9) is obtained by averaging over a few grating periods. Using (9) and (A9), one may show that we have the following equation for a second-order gain grating:

$$\left\langle \widetilde{f}^i_\omega(z)\widetilde{f}^{j*}_{\omega'}(z')\right\rangle = 2D_{\widetilde{f}^i\widetilde{f}^{j*}}\delta(\omega-\omega')\delta(z-z') \tag{A10}$$

where $i,j=A$ or B, and

$$2D_{\widetilde{f}^A\widetilde{f}^{A*}} = 2D_{\widetilde{f}^B\widetilde{f}^{B*}} = \frac{\hbar\omega_0^3 n(z)\Gamma g_{\rm av}(z)n_{\rm sp}}{\varepsilon_0 c^3\xi(\Phi_\omega)} \tag{A11}$$

$$2D_{\widetilde{f}^A\widetilde{f}^{B*}} = 2D^*_{\widetilde{f}^B\widetilde{f}^{A*}} = \frac{4\hbar\omega_0^3 n(z)\kappa_g e^{j2\theta(z)}n_{\rm sp}}{\varepsilon_0 c^3\xi(\Phi_\omega)}. \tag{A12}$$

In the derivation of (A12) for a symmetric second-order gain grating, we have used [21]

$$\Gamma g_2(z) = \Gamma g_{-2}(z) = 2\kappa_g. \tag{A13}$$

Since (9) does not uniquely specify $\widetilde{f}^A_\omega(z)$ and $\widetilde{f}^B_\omega(z)$ in terms of $\widetilde{F}_\omega(z)$, the derivations of (A8), (A11), and (A12) mostly rely on physical intuition rather than mathematical rigor.

APPENDIX B

To solve (31), we assume that

$$\widetilde{\mathbf{G}}_{1,\omega}(z,z') = \begin{cases}\widetilde{\mathbf{G}}^+_{1,\omega}(z,z'), & z>z'\\ \widetilde{\mathbf{G}}^-_{1,\omega}(z,z'), & z<z'\end{cases} \tag{B1}$$

where $\widetilde{\mathbf{G}}^+_{1,\omega}(z,z')$ and $\widetilde{\mathbf{G}}^-_{1,\omega}(z,z')$ satisfy the homogeneous equation obtained from (31) by setting its right-hand side equal to $[0\quad 0]^{\rm T}$.

Let

$$\widetilde{\mathbf{G}}^\pm_{1,\omega}(z,z') = \begin{bmatrix}\widetilde{g}^{A\pm}_{1,\omega}(z,z')\\ \widetilde{g}^{B\pm}_{1,\omega}(z,z')\end{bmatrix}. \tag{B2}$$

By integrating (31) from $z = z' - \varepsilon$ to $z = z' + \varepsilon$ $(\varepsilon \to 0)$, we get

$$\begin{bmatrix} \widetilde{g}_{1,\omega}^{A+}(z',z') \\ \widetilde{g}_{1,\omega}^{B+}(z',z') \end{bmatrix} - \begin{bmatrix} \widetilde{g}_{1,\omega}^{A-}(z',z') \\ \widetilde{g}_{1,\omega}^{B-}(z',z') \end{bmatrix} = \begin{bmatrix} 0 \\ -1 \end{bmatrix}. \tag{B3}$$

On the other hand, one may write

$$\begin{bmatrix} \widetilde{g}_{1,\omega}^{A+}(z',z') \\ \widetilde{g}_{1,\omega}^{B+}(z',z') \end{bmatrix} = \widetilde{\mathbf{T}}_\omega(z',L) \begin{bmatrix} 1 \\ r_L \end{bmatrix} \widetilde{g}_{1,\omega}^{A+}(L,z') \tag{B4}$$

$$\begin{bmatrix} \widetilde{g}_{1,\omega}^{A-}(z',z') \\ \widetilde{g}_{1,\omega}^{B-}(z',z') \end{bmatrix} = \widetilde{\mathbf{T}}_\omega(z',0) \begin{bmatrix} r_0 \\ 1 \end{bmatrix} \widetilde{g}_{1,\omega}^{B-}(0,z') \tag{B5}$$

where r_0 and r_L are the field reflectivity at $z = 0$ and $z = L$, respectively, and $\widetilde{\mathbf{T}}_\omega(z_2, z_1)$ is the transfer matrix that relates the amplitudes of the forward and backward waves at $z = z_2$ to those at $z = z_1$. The general form of $\widetilde{\mathbf{T}}_\omega(z_2, z_1)$ is given as follows:

$$\widetilde{\mathbf{T}}_\omega(z_2,z_1) = \begin{bmatrix} \widetilde{T}_\omega^{11}(z_2,z_1) & \widetilde{T}_\omega^{12}(z_2,z_1) \\ \widetilde{T}_\omega^{21}(z_2,z_1) & \widetilde{T}_\omega^{22}(z_2,z_1) \end{bmatrix} \tag{B6}$$

where

$$\widetilde{T}_\omega^{11}(z_2,z_1) = \cosh[\gamma(z_2 - z_1)] + \widetilde{K}_\omega^{11}\gamma^{-1}\sinh[\gamma(z_2 - z_1)] \tag{B7}$$

$$\widetilde{T}_\omega^{12}(z_2,z_1) = \widetilde{K}_\omega^{12}\gamma^{-1}\sinh[\gamma(z_2 - z_1)] \tag{B8}$$

$$\widetilde{T}_\omega^{21}(z_2,z_1) = -\widetilde{K}_\omega^{21}\gamma^{-1}\sinh[\gamma(z_2 - z_1)] \tag{B9}$$

$$\widetilde{T}_\omega^{22}(z_2,z_1) = \cosh[\gamma(z_2 - z_1)] - \widetilde{K}_\omega^{11}\gamma^{-1}\sinh[\gamma(z_2 - z_1)] \tag{B10}$$

and

$$\gamma = \sqrt{\left[\widetilde{K}_\omega^{11}\right]^2 - \widetilde{K}_\omega^{12}\widetilde{K}_\omega^{21}}. \tag{B11}$$

Substituting (B4) and (B5) into (B3) leads to equations for $\widetilde{g}_{1,\omega}^{A+}(L,z')$ and $\widetilde{g}_{1,\omega}^{B-}(0,z')$ as follows:

$$\widetilde{\mathbf{T}}_\omega(z',L)\begin{bmatrix} 1 \\ r_L \end{bmatrix}\widetilde{g}_{1,\omega}^{A+}(L,z') - \widetilde{\mathbf{T}}_\omega(z',0)\begin{bmatrix} r_0 \\ 1 \end{bmatrix}\widetilde{g}_{1,\omega}^{B-}(0,z') = \begin{bmatrix} 0 \\ -1 \end{bmatrix}. \tag{B12}$$

It should be noted that (B12) is also valid for $z' = 0$ and $z' = L$.

To obtain $\widetilde{g}_{1,\omega}^{B-}(0,z')$, we multiply both sides of (B12) by $[-r_L \quad 1] \times \widetilde{\mathbf{T}}_\omega^{-1}(z',L)$, and we get

$$\widetilde{g}_{1,\omega}^{B-}(0,z') = \widetilde{D}_\omega^{-1}[-r_L \quad 1]\widetilde{\mathbf{T}}_\omega^{-1}(z',L)\begin{bmatrix} 0 \\ -1 \end{bmatrix} \tag{B13}$$

where

$$\widetilde{D}_\omega = [r_L \quad -1]\widetilde{\mathbf{T}}_\omega(L,0)\begin{bmatrix} r_0 \\ 1 \end{bmatrix}. \tag{B14}$$

In deriving (B13) and (B14), we have used the following identities for the transfer matrices:

$$\widetilde{\mathbf{T}}_\omega^{-1}(z_i,z_j) = \widetilde{\mathbf{T}}_\omega(z_j,z_i) \tag{B15}$$

and

$$\widetilde{\mathbf{T}}_\omega(z_i,z_j)\widetilde{\mathbf{T}}_\omega(z_j,z_k) = \widetilde{\mathbf{T}}_\omega(z_i,z_k). \tag{B16}$$

In a similar fashion, from (B12), it follows that

$$\widetilde{g}_{1,\omega}^{A+}(L,z') = \widetilde{D}_\omega^{-1}[-1 \quad r_0]\widetilde{\mathbf{T}}_\omega^{-1}(z',0)\begin{bmatrix} 0 \\ -1 \end{bmatrix} \tag{B17}$$

where we have used

$$[-1 \quad r_0]\widetilde{\mathbf{T}}_\omega(0,L)\begin{bmatrix} 1 \\ r_L \end{bmatrix} = [r_L \quad -1]\widetilde{\mathbf{T}}_\omega(L,0)\begin{bmatrix} r_0 \\ 1 \end{bmatrix}. \tag{B18}$$

Equation (B18) is obtained by using (B15) and noting that $|\widetilde{\mathbf{T}}_\omega(z_i,z_j)| = 1$.

After obtaining $\widetilde{g}_{1,\omega}^{B-}(0,z')$ and $\widetilde{g}_{1,\omega}^{A+}(L,z')$, one may obtain $\widetilde{\mathbf{G}}_{1,\omega}^{\pm}(z,z')$ by the transfer matrices. More precisely

$$\widetilde{\mathbf{G}}_{1,\omega}^{+}(z,z') = \widetilde{\mathbf{T}}_\omega(z,L)\begin{bmatrix} 1 \\ r_L \end{bmatrix}\widetilde{g}_{1,\omega}^{A+}(L,z') \tag{B19}$$

and

$$\widetilde{\mathbf{G}}_{1,\omega}^{-}(z,z') = \widetilde{\mathbf{T}}_\omega(z,0)\begin{bmatrix} r_0 \\ 1 \end{bmatrix}\widetilde{g}_{1,\omega}^{B-}(0,z'). \tag{B20}$$

For $z' = 0$, we have $\widetilde{\mathbf{G}}_{1,\omega}(z,0) = \widetilde{\mathbf{G}}_{1,\omega}^{+}(z,0)$, whereas for $z' = L$, we have $\widetilde{\mathbf{G}}_{1,\omega}(z,L) = \widetilde{\mathbf{G}}_{1,\omega}^{-}(z,L)$.

In a similar fashion, $\widetilde{\mathbf{G}}_{2,\omega}(z,z')$ can be obtained by replacing $[0 \quad -1]^{\mathrm{T}}$ with $[1 \quad 0]^{\mathrm{T}}$ and repeating the above steps. The validity of (37) can also be checked using these explicit expressions for $\widetilde{\mathbf{G}}_{1,\omega}(z,z')$ and $\widetilde{\mathbf{G}}_{2,\omega}(z,z')$.

It should be emphasized that the spatial hole burning effect can be included by dividing the laser cavity into M sections such that the carrier distribution in each section is assumed to be uniform. The transfer matrix that relates the amplitudes of the forward and backward waves at $z = z_2$ to those at $z = z_1$ is then considered as the product of the corresponding transfer matrices of those sections that exist in the interval $z_1 \le z \le z_2$.

ACKNOWLEDGMENT

The authors would like to thank the referees for their comments.

REFERENCES

[1] W. Streifer, R. D. Burnham, and D. R. Scifres, "Radiation losses in distributed feedback lasers and longitudinal mode selection," *IEEE J. Quantum Electron.*, vol. QE-12, no. 11, pp. 737–739, Nov. 1976.

[2] R. Kazarinov and C. H. Henry, "Second-order distributed feedback lasers with mode selection provided by first-order radiation losses," *IEEE J. Quantum Electron.*, vol. QE-21, no. 2, pp. 144–150, Feb. 1985.

[3] C. H. Henry, R. Kazarinov, R. Logan, and R. Yen, "Observation of destructive interference in the radiation loss of second-order distributed feedback lasers," *IEEE J. Quantum Electron.*, vol. QE-21, no. 2, pp. 151–154, Feb. 1985.

[4] C. J-I. Kinoshita, "Axial profile of grating coupled radiation from second-order DFB lasers with phase shift," *IEEE J. Quantum Electron.*, vol. 26, no. 3, pp. 407–412, Mar. 1990.

[5] N. W. Carlson, S. K. Kuen, R. Amantea, D. P. Bour, G. A. Evans, and E. A. Vangieson, "Mode discrimination in distributed feedback grating surface emitting lasers containing a buried second-order grating," *IEEE J. Quantum Electron.*, vol. 27, no. 6, pp. 1746–1752, Jun. 1991.

[6] S. F. Yu, L. M. Zhang, R. G. S. Plumb, and J. E. Carroll, "Effect of external reflectors on radiation profile of grating coupled surface emitting lasers," *Proc. Inst. Elect. Eng.—J. Optoelectron.*, vol. 140, no. 1, pp. 30–38, Feb. 1993.
[7] S. H. Macomber and J. S. Mott, "Chirped grating surface emitting distributed feedback semiconductor laser," U.S. Patent 5 241 556, Aug. 31, 1993.
[8] Y. Hirayama, M. Funemizu, M. Tohayama, M. Morinaga, K. Takaoka, K. Inoue, and M. Ohashi, "Grating coupled surface emitting device," U.S. Patent 5 970 081, Oct. 19, 1999.
[9] M. Kasraian and D. Botez, "Single-lobe operation of surface-emitting complex-coupled second-order distributed-feedback diode lasers," in *Proc. IEEE Lasers Electro-Optics Annu. Meetings*, Oct. 1995, vol. 1, pp. 292–293.
[10] M. Kasraian, J. Lopez, and D. Botez, "Antiphase complex-coupled surface-emitting distributed feedback diode lasers with absorptive gratings," *IEEE Photon. Technol. Lett.*, vol. 10, no. 1, pp. 27–29, Jan. 1998.
[11] S. Li, G. Witjaksono, S. Macomber, and D. Botez, "Analysis of surface-emitting second-order distributed feedback lasers with central grating phase shift," *IEEE J. Sel. Topics Quantum Electron.*, vol. 9, no. 5, pp. 1153–1165, Sep./Oct. 2003.
[12] H. Wenzel, "Green's function based simulation of the optical spectrum of multisection lasers," *IEEE J. Sel. Topics Quantum Electron.*, vol. 9, no. 3, pp. 865–871, May/Jun. 2003.
[13] C. H. Henry, "Theory of spontaneous emission noise and open resonators and its application to lasers and optical amplifiers," *J. Lightw. Technol.*, vol. LT-4, no. 3, pp. 288–297, Mar. 1986.
[14] W. Streifer, D. R. Scifres, and R. Burnham, "Coupled wave analysis of DFB and DBR lasers," *IEEE J. Quantum Electron.*, vol. QE-13, no. 4, pp. 134–141, Apr. 1977.
[15] A. M. Shams-Zadeh-Amiri, X. Li, and W.-P. Huang, "Second- and higher order resonant gratings with gain or loss—Part I: Green's function analysis," *IEEE J. Quantum Electron.*, vol. 36, no. 12, pp. 1421–1430, Dec. 2000.
[16] C. H. Henry, "Theory of the linewidth of semiconductor lasers," *IEEE J. Quantum Electron.*, vol. QE-18, no. 2, pp. 259–264, Feb. 1982.
[17] K. Hoffman and R. Kunze, *Linear Algebra*. Englewood Cliffs, NJ: Prentice-Hall, 1971.
[18] R. G. Baets, K. David, and G. Morthier, "On the distinctive features of gain-coupled DFB lasers and DFB lasers with second-order grating," *IEEE J. Quantum Electron.*, vol. 29, no. 6, pp. 1792–1798, Jun. 1993.
[19] A. M. Shams-Zadeh-Amiri, J. Hong, X. Li, and W.-P. Huang, "Second and higher order resonant gratings with gain or loss—Part II: Designing complex-coupled DFB lasers with second-order gratings," *IEEE J. Quantum Electron.*, vol. 36, no. 12, pp. 1431–1437, Dec. 2000.
[20] D. M. Adams, I. Woods, J. K. White, R. Finlay, and D. Goodchild, "Gain-coupled DFB lasers with truncated quantum well second-order gratings," *Electron. Lett.*, vol. 37, no. 25, pp. 1520–1521, Dec. 6, 2001.
[21] K. David, J. Buss, G. Morthier, and R. Baets, "Coupling coefficients in gain-coupled DFB lasers: Inherent compromise between coupling strength and loss," *IEEE Photon. Technol. Lett.*, vol. 3, no. 5, pp. 439–441, May 1991.

Ali M. Shams-Zadeh-Amiri (M'00) received the B.S. and M.S. degrees from the University of Tehran, Tehran, Iran, and the Ph.D. degree from the University of Waterloo, Waterloo, ON, Canada, in 1987, 1990, and 1997, respectively, all in electrical engineering.

Until 1998, he was with Nortel Networks, Ottawa, ON, where he conducted research on multiple-quantum-well DFB lasers with a second-order gain grating for advanced optical communications systems. From 1999 to 2000, he was with the Department of Electrical and Computer Engineering, University of Waterloo, as a Research Assistant Professor, conducting research on dielectric resonators and teaching courses in electromagnetic theory. Since 2000, he has been with Photonami Corporation, Richmond Hill, ON, as a Research Scientist. He is currently a Senior Laser Designer involved in the research and development of surface-emitting DFB lasers for optical switches in metropolitan area networks. He is the holder of four U.S. and international patents. His research interests include multiple-quantum-well DFB lasers in general and surface-emitting DFB lasers in particular, integrated optics, numerical simulation of optoelectronic devices, fiber gratings, RF/microwave, dielectric resonators, and electromagnetic theory.

Wei Li (M'00) received the B.S degree in physics from Jilin University, Changchun, China, the M.S. degree in physics from Nankai Institute of Mathematics, Nankai University, Tianjin, China, and the Ph.D. degree in electrical engineering from University of Waterloo, Waterloo, ON, Canada, in 1989, 1992, and 2000, respectively.

In 1999, he joined Apollo Photonics Inc., Burlington, ON, as a Research Engineer, where he was also an Natural Sciences and Engineering Research Council (NSERC) Industry Research Fellow. He was in charge of computer-aided-design simulation software development of active/functional components for fiber-optic communication systems and advanced material/device design including strained quantum wells, semiconductor laser diodes (Fabry–Pérot (FP), DFB, and distributed Bragg reflector), semiconductor optical amplifiers, electroabsorbtive modulators, and other integrated devices. In 2001, he joined Photonami Corporation, Richmond Hill, ON, as a Research Scientist and worked on an innovative surface-emitting DFB laser for metropolitan/long-haul optical networks. He was also the coinventor of the device. Since 2003, he has been with the Department of Chemistry and Engineering Physics, University of Wisconsin-Platteville, as an Assistant Professor. His current research interests include optoelectronic devices for fiber-optic communication systems, quantum electronics, quantum effects of nanoscale structures/devices, and nanophotonics.

Hans Wenzel received the diploma and doctoral degrees from Humboldt University, Berlin, Germany, in 1986 and 1991, respectively, all in physics. His thesis dealt with electrooptical modeling of semiconductor lasers.

From 1991 to 1994, he was involved in a research project on the three-dimensional simulation of DFB lasers. Since 1994, he has been with the Ferdinand-Braun-Institut für Höchstfrequenztechnik, Berlin, where he is involved in the development of high-power semiconductor lasers. His main research interests include analysis, modeling, and simulation of optoelectronic devices.

Xun Li (M'93–SM'04) received the B.S. degree from Shandong University, Jinan, China; the M.S. degree from the Research Institute of Posts Telecommunications, Wuhan, China; and the Ph.D. degree from Northern Jiaotong University, Beijing, China, in 1982, 1984, and 1988, respectively.

In 1988, he was a Professor at the Lightwave Technology Institute, Northern Jiaotong University. From 1993 to 1999, he was a Research Assistant Professor at the Department of Electrical and Computer Engineering, University of Waterloo, Waterloo, ON, Canada. In 1999, he joined the Faculty of Engineering at McMaster University, Hamilton, ON, and is currently an Associate Professor. His research interests include optical fiber communication systems and quantum electronics with emphasis on computer-aided modeling, simulation, and design of optoelectronic devices such as semiconductor lasers and amplifiers and their applications to optical fiber communication systems and networks.